Applying the Exponential Chebyshev Inequality to the Nondeterministic Computation of Form Factors

GLADIMIR V. G. BARANOSKI   JON G. ROKNE   GUANGWU XU

Department of Computer Science, The University of Calgary, 2500 University Dr. N.W., Calgary, Alberta, T2N 1N4, Canada

Tecnical Report 99/638/01

Abstract
The computation of the fraction of radiation power that leaves a surface and arrives at another, which is specified by the form factor linking both surfaces, is central to radiative transfer simulations. Although there are several approaches that can be used to compute form factors, the application of nondeterministic methods is becoming increasingly important due to the simplicity of their procedures and their wide range of applications. These methods compute form factors implicitly through the application of standard Monte Carlo techniques and ray casting algorithms. Their accuracy and computational costs are, however, highly dependent on the ray density used in the computations. In this paper a mathematical bound, based on probability theory, is proposed to determine the number of rays needed to obtain asymptotically convergent estimates for form factors in a computationally efficient stochastic process. Specifically, the exponential Chebyshev inequality is introduced to the radiative transfer field in order to determine the ray density required to compute form factors with a high reliability/cost ratio. Numerical experiments are provided which illustrate the validity and usefulness of the proposed bound.

1. Introduction

A form factor, also called configuration or view factor [1], indicates how a surface "sees" another surface. In other words, it specifies the fraction of radiant power that leaves a surface and arrives at another. Form factors depend on the shape and relative orientation of the surfaces as well as on the presence of obstacles between them. Although there is no closed form solution for the form factors, there are useful analytical formulae for simple geometrical configurations [1, 2, 3, 4, 5, 6, 7, 8, 9, 10, 11]. However, these formulae are usually not general enough to be used in radiative transfer applications involving complex geometrical configurations. Moreover, the existing analytical formulae are oftentimes complex, which makes them prone to roundoff and truncation errors. For these reasons, several numerical methods have been developed to compute form factors. Generally speaking, these methods can be divided into two groups: deterministic and nondeterministic.

The deterministic methods for the computation of form factor between surfaces are usually based on the application of mathematical tools such as contour integration [9] or Gaussian quadrature [12]. In order to apply these tools it is required that both surfaces have certain properties such that a regular grid or subdivision can be found on them or along their boundaries. Although it is possible to relax the above requirement, the algorithms will then be correspondingly complex. The nondeterministic methods, based on the use of Monte Carlo techniques [13] and ray casting algorithms [14, 15], do not require a regular grid on the surface. This aspect allows the application of these methods to wide variety of geometric configurations. Their application requires only the selection of the origin and the direction of sample rays according to an appropriate probability criteria. These methods consist basically of the determination of the numerical value of an estimand [13], or expected value, to which the fraction of the radiation transferred between an differential element and a surface, or between two surfaces, converges. This estimand will correspond to the form factor between the two elements. For a comprehensive literature review of the application of Monte Carlo based methods in the solution of radiative transfer problems, such as the computation of form factors, the reader is referred to Ref. 29.

In applications involving Monte Carlo techniques variance is used as a measure of dispersion around the estimand [13]. Variance is defined as the square of the standard deviation, which, in turn, indicates the absolute deviation from the estimand. Due to their stochastic nature the nondeterministic methods may sometimes provide estimates with low variance with respect to the estimand in the early stages of the simulation, *i.e.* after using a small number of sample rays. Since the value of the estimand is unknown before the simulation, these earlier estimates are not reliable, and estimates within the region of asymptotic convergence of the estimand are, therefore, desired. In fact, if one knew *a priori* the value of the estimand for a given geometric configuration, there would be no point in carrying out the numerical computation of the form factor. To ensure that the estimates regarding a given geometrical configuration are within the asymptotic convergence region, a brute-force approach, which consists of using a very large number of sample rays, can be applied. However, the application of this strategy results in a high computational overhead in terms of processing time.

In this paper we present a bound for the least number of sample rays required to obtain estimates that lie within the region of asymptotic convergence of the estimand with high probability, and, consequently, substantially reduce the processing time. For the reason mentioned earlier, the determination of an appropriate ray density, or sample size [13], shall not depend on the knowledge about the value of the estimand or on its variance. In order to fulfill this guideline we present a mathematical criterion derived from a probability concept, namely the exponential Chebyshev inequality [16, 17], and adapt it to the requirements of radiative transfer simulations. Practical experiments involving different geometrical configurations are shown to illustrate its suitability to the nondeterministic computation of form factors. Moroever, theoretical and numerical comparisons with ray densities provided by the ordinary Chebyshev inequality [17, 18, 19] are also provided with the same purpose.

After we completed the research presented in this paper, we learned that the connection between form factor computation and probability inequalities, such as the ordinary Chebyshev inequality, was noted by Pellegrini [20]. However, his use of these inequalities is different from the one performed in this paper. In his paper, Pellegrini presents a Monte Carlo algorithm to compute approximations of form factors using the theory of integral geometry [21]. He uses the inequalities to provide an upper bound on the running time of his algorithm and an upper bound on the absolute approximation error of each form factor computed through it. Besides the differences in the application of the inequalities, Pelligrini does not include practical experiments in his research. In this context, although our research was developed independently of the research done by Pellegrini, some of its aspects might also be viewed as a more thorough examination of some of the ideas presented in his paper. As mentioned above, we also refer to the ordinary Chebyshev inequality in comparisons involving the exponential Chebyshev inequality. Our investigation, however, is not limited to theoretical aspects, but involves also the examination of practical issues related to the application of these inequalities to form factor computation.

The remainder of this paper is organized as follows. The next section provides an overview of the formulation of nondeterministic methods for form factor computation. Section 3 introduces the exponential Chebyshev inequality, and discusses its application to form factor computation. Section 4 describes the performance criterion and the geometrical configurations used in the numerical experiments performed to evaluate the applicability of the proposed bound. Section 5 discusses the results of these experiments. Finally, the paper closes with a summary of the main conclusions and with directions for future research.

2. Statement of Nondeterministic Methods for Form Factor Computation

For the following presentation we consider only finite Lambertian† elements (differential ones or surfaces). Moreover, light propagation is described in terms of ray or geometrical optics, where light is assumed to be composed of non-interacting straight rays, each of them carrying a certain amount of energy [23].

2.1. General Concepts

The form factor linking two elements i and j represents the inverse ratio between the radiant power leaving the emitter element i, denoted by Φ_i, and the radiant power arriving at the receiver element j, denoted by Φ_{ij}, and it is given by:

$$F_{ij} = \frac{\Phi_{ij}}{\Phi_i} \tag{1}$$

As mentioned earlier, nondeterministic methods implicitly estimate F_{ij} by using Monte Carlo techniques [13]. Since we are considering only diffuse elements, we know that the element i reflects/emits radiant power in a cosine distribution, which in turn allow us to divide Φ_i into N packets or rays. Each ray is sent in a random direction. As pointed out by Shirley [24], these

† Lambertian or ideal diffuse surfaces appear equally bright from all viewing angles because they have a constant spectral radiance at all viewing angles under steady lighting conditions [22].

directions should have a cosine density, rather than being uniformly random. If a ray hits the element j, *i.e.* the element j is seen by the element i in the direction that the ray is sent, the radiant power carried by the ray is fully transferred to it.

Considering a total number of N rays, and assuming that each ray carries the same amount of radiant power and the total radiant power to be shot is Φ_i, then, as stated by Shirley [22, 25], the radiant power carried by each ray is given by:

$$\Phi_{ray}(\lambda) = \frac{\Phi_i}{N} \tag{2}$$

Therefore, if m rays hit the element j, the form factor linking i and j can be represented by:

$$F_{ij} = \frac{m\ \Phi_{ray}}{N\ \Phi_{ray}} \tag{3}$$

or simply:

$$F_{ij} = \frac{m}{N} \tag{4}$$

Although the concepts presented above represent the kernel of nondeterministic methods for form factor computation, one can find different algorithms in the literature [26] according to the strategies applied to select the origin and the direction of the sample rays. In the next section we discuss this issue, and outline strategies commonly used to generate sample rays.

2.2. Sampling Strategies

2.2.1. Emitter Sampling

For geometric configurations in which the emitter element is represented by a differential element, all sample rays have the same origin. When the emitter is represented by a finite surface, however, sample points are randomly chosen to represent the origin of the rays. In order to apply Monte Carlo techniques these points must be generated according to a *probability density function* (*pdf*) [13]. Before proceeding with this discussion, we shall briefly review some relevant definitions.

If a random variable ς ranges over some region Ω, then the probability that ς will take on a value in some subregion $\Omega_i \subset \Omega$ is given by:

$$\Gamma(\varsigma \in \Omega_i) = \int_{\varsigma' \in \Omega_i} pdf(\varsigma')\ d\mu(\varsigma') \quad (pdf : \Omega \to \Re^1) \tag{5}$$

where $\Gamma(event)$, also called cumulative distribution function [13], is the probability that the *event* is true [22]. In ray casting applications Ω is typically an area ($d\mu = dA = dx\ dy$) or a set of directions ($d\mu = d\omega = sin\alpha\ d\alpha\ d\beta$).

Consider a one-dimensional *pdf* represented by a function $f(z)$ and defined over the interval $z \in [a,b]$. We can generate random numbers ζ_i that have a density f from a set of uniformly distributed random numbers ξ_i, where $\xi_i \in [0,1]$, using a warping function W such that:

$$\zeta_i = W(\xi_i) \tag{6}$$

where W is given by the inverse of the corresponding cumulative distribution function, *i.e.* $W = \Gamma^{-1}$. For the one-dimensional *pdf* defined above, the corresponding cumulative distribution function is given by:

$$\Gamma(z) = \int_a^x f(z')\ d\mu(z') \tag{7}$$

For a two-dimensional *pdf*, we need a two-dimensional cumulative distribution function $\Gamma(x,y)$. In this case, if $\Gamma(x,y)$ is separable, then the one-dimensional techniques can be used on each dimension to determine the warping function. We examine this possibility in more detail in the next section.

In the experiments presented in Sec. 5 regarding the form factor between two squares (Sec. 4.2.6), the emitter element is represented by two triangles, T_1 and T_2. For each ray we generate a uniformly distributed random number ξ in the interval $[0,1]$. If $\xi \geq 0.5$, then we choose a random point on T_1 as the origin. Otherwise, we choose a point on T_2.

In order to choose a random point q on a triangle defined by the vertices q_0, q_1 and q_2, the following *pdf* [27] can be used:

$$pdf(q) = \frac{1}{A} \tag{8}$$

where A corresponds to the area of the triangle.

In this case, a random point q on the triangle is given by:

$$q = q_0 + s(q_1 - q_0) + t(q_2 - q_0) \tag{9}$$

where s and t are obtained using the following warping function [27]:

$$(s,t) = (1 - \sqrt{1-\xi_1}, (1-s)\xi_2) \tag{10}$$

where ξ_1 and ξ_2 are uniformly distributed random numbers in the interval $[0,1]$.

2.2.2. Directional Sampling

To simulate the distribution of the rays sent by a diffuse emitter element, we also use warping functions. In this case, the *pdf* corresponds to a cosine distribution [22, 28], and it is given by:

$$pdf(\alpha,\beta) = \frac{1}{\pi} cos\alpha \tag{11}$$

where α corresponds to the polar angle with respect to the normal of the element, and β corresponds to the azimuthal angle around the normal of the element. These angles correspond to angular displacements used to perturb the emitted rays.

The cumulative density function for the *pdf* expressed by Eq. (11) is given by:

$$\Gamma(\alpha,\beta) = \int_0^\beta \int_0^\alpha \frac{cos\alpha'}{\pi}\ sin\alpha'\ d\alpha'\ d\beta' \tag{12}$$

Since the *pdf* expressed by Eq. (11) is separable, as mentioned earlier, one-dimensional derivation techniques can be applied on each dimension to find the warping function used to generated the corresponding angular displacements. Solving Eq. (12) in the dimension associated with α results in:

$$\int_0^\alpha 2\ cos\alpha'\ sin\alpha'\ d\alpha' = 2\left[-\frac{cos^2\alpha'}{2}\right]_0^\alpha = 2\left(-\frac{cos^2\alpha}{2} + \frac{1}{2}\right) = -cos^2\alpha\ +\ 1 \tag{13}$$

which means that:

$$-cos^2\alpha\ +\ 1 = \xi_1 \tag{14}$$

or:

$$\alpha = arccos(\sqrt{1-\xi_1}) \tag{15}$$

where ξ_1 is an uniformly distributed random number in the interval $[0,1]$.

Solving for the dimension associated with β gives:

$$\int_0^\beta \frac{1}{2\pi}\ d\beta' = \frac{\beta}{2\pi} \tag{16}$$

which means that:

$$\frac{\beta}{2\pi} = \xi_2 \tag{17}$$

or:

$$\beta = 2\pi\xi_2 \tag{18}$$

where ξ_2 is an uniformly distributed random number in the interval $[0,1]$.

Therefore, the corresponding warping function used to generate the angular displacements represented by the angles α and β is given by:

$$(\alpha,\beta) = (arccos(\sqrt{1-\xi_1}), 2\pi\xi_2) \tag{19}$$

3. Ray Density Bound

As mentioned earlier, we denote the total number of sample rays, or the ray density, by N. However, for the sake of compactness, we may also represented it by $\log N$ (base 10). The main question to be addressed when applying a nondeterministic method to compute form factors is how many rays should be cast by the emitter element; that is, how large should N be.

Clearly, using a sufficiently large number of sample rays, one will have a high probability to obtain estimates within the region of convergence of the expected value of the form factor being computed. However, as shown by numerical experiments presented in Sec. 5, the processing time grows rapidly according to the total number of sample rays N.

The purpose of the following discussion is to determine a satisfactory bound for N such that we can obtain estimates of the form factor between diffuse elements with a high reliability/cost ratio (Sec. 4.1). In order words, we want to obtain estimates within the region of asymptotic convergence and reduce the computational time. Before getting to the specifics of the criterion proposed in this paper for selecting a satisfactory bound for N, we review some relevant definitions and concepts.

3.1. Bernoulli Theorem and Chebyshev Inequality

A random variable ζ that takes two values 1 and 0 with probabilities p ("success") and q ("failure"), where $p+q=1$, is called a Bernoulli random variable [16]. A probabilistic model of k independent sampling experiments with two possible outcomes occurring with probabilities p and q is called a Bernoulli trial [16, 29, 30].

Suppose that $\zeta_1, \zeta_2, \ldots, \zeta_k$ are independent Bernoulli variables. The expectation of a Bernoulli variable ζ_i is given by:

$$E(\zeta_i) = p \tag{20}$$

As stated by Shiryaev [16], if we define the sum of k Bernoulli random variables as:

$$S_k = \sum_{i=1}^{k} \zeta_i \tag{21}$$

it follows that:

$$E(S_k) = kp \tag{22}$$

As stated by Chiang [18], for sufficiently large k, the relative frequency $\frac{S_k}{k}$ becomes and remains close to p with a probability of one. Jacob Bernoulli in his posthumous book *Ars Conjectandi* (1713) published a theorem, whose proof can be found in the book by Uspensky [30], that formally describes this fact. The Bernoulli theorem states that, for every strip of width $\varepsilon > 0$ and error tolerance $\delta > 0$, there is a number G such that, for $k = G+1, G+2, \ldots$,

$$P\left\{ \left| \frac{S_k}{k} - p \right| \geq \varepsilon \right\} > 1 - \delta \tag{23}$$

where $P\{w\}$ means the probability of w.

The particle transport simulation using Monte Carlo techniques can be seen as a Bernoulli trial [31, 32]. In this context a general result of probability theory, known as the Chebyshev inequality [17, 18, 19], can be used to determine the number of samples needed to obtain estimates with a certain error tolerance in a strip of width ε. This inequality states that:

$$P\{\zeta \geq \varepsilon\} \leq \frac{E(\zeta)}{\varepsilon} \qquad \forall \varepsilon > 0 \tag{24}$$

From the Chebyshev inequality it can be shown [16] that:

$$P\left\{ \left| \frac{S_k}{k} - p \right| \geq \varepsilon \right\} \leq \frac{pq}{k\varepsilon^2} \leq \frac{1}{4k\varepsilon^2} \tag{25}$$

Recall from probability theory that:

$$P\{|w| < \varepsilon\} = 1 - P\{|w| \geq \varepsilon\} \tag{26}$$

Hence, we can rewrite the inequality given by Eq. (25) as:

$$P\left\{ \left| \frac{S_k}{k} - p \right| < \varepsilon \right\} \geq 1 - \frac{1}{4k\varepsilon^2} \tag{27}$$

The error tolerance in an estimation is a given parameter (usually small). Theoretically δ is a positive number such that:

$$\delta \geq 1 - P\left\{\left|\frac{S_k}{k} - p\right| < \varepsilon\right\} \tag{28}$$

Then, to satisfy the above inequality, it is required that:

$$\delta \geq \frac{1}{4k\varepsilon^2} \tag{29}$$

Therefore, from the Chebyshev inequality, the least number of sampling experiments required to obtain estimates with an error tolerance δ is given by:

$$k_c = \left\lceil \frac{1}{4\varepsilon^2\delta} \right\rceil \tag{30}$$

3.2. Applying the Exponential Chebyshev Inequality to the Computation of Form Factors

The "exponential form" of the Chebyshev inequality, known as the exponential Chebyshev inequality [16], can used to obtain a more precise bound for the smallest number of sampling experiments required. Assuming $w \geq 0$ and $\nu > 0$, the exponential Chebyshev inequality states that:

$$P\{w \geq \varepsilon\} = P\{e^{\nu w} \geq e^{\nu\varepsilon}\} \leq E\{e^{\nu(w-\varepsilon)}\} \tag{31}$$

From the exponential Chebyshev inequality it can be shown [16] that:

$$P\left\{\left|\frac{S_k}{k} - p\right| \geq \varepsilon\right\} \leq 2e^{-2k\varepsilon^2} \tag{32}$$

Using Eq. (26) it follows that:

$$P\left\{\left|\frac{S_k}{k} - p\right| < \varepsilon\right\} \geq 1 - 2e^{-2k\varepsilon^2} \tag{33}$$

From a reasoning similar to the one used to obtain the inequality given by Eq. (29), it follows that:

$$\delta \geq 2e^{-2k\varepsilon^2} \tag{34}$$

Hence, from the exponential Chebyshev inequality, the least number of sampling experiments need to obtain estimates with an error tolerance δ is given by:

$$k_e = \left\lceil \frac{\ln(\frac{2}{\delta})}{2\varepsilon^2} \right\rceil \tag{35}$$

As shown by Shiryaev [16], using the theory of limits [16], it is possible to compare the bound k_c provided by the ordinary Chebyshev inequality with the bound k_e provided by the exponential Chebyshev inequality:

$$\lim_{\delta \to 0} \frac{k_c(\delta)}{k_e(\delta)} = \lim_{\delta \to 0} \frac{1}{2\delta \ln(\frac{2}{\delta})} = \infty \tag{36}$$

It is clear from the previous expression that, when $\delta \to 0$, k_e is tighter than k_c for radiative transfer applications involving high accuracy requirements, *i.e.* low values δ. Moreover, the figures presented in Table 1 show that, even for applications involving relatively low accuracy requirements, *i.e.* relative large values for δ, the bound derived from the exponential Chebyshev inequality results in a number of sampling experiments considerably smaller than the number given by the bound derived from the ordinary Chebyshev inequality. In Sec. 5 we present numerical experiments that illustrate the applicability of the bound derived from the exponential Chebyshev inequality in the computation of form factors through nondeterministic methods, and highlight the significant time savings that can be obtained from its application. Before going further in this discussion however, we shall describe how the probability concepts presented so far fit into the computation of diffuse form factors through nondeterministic methods.

Recall that each ray sent by the emitter element either hits the receiver element, which will receive all of its power, or

Table 1: *Comparison of bounds on the number of sampling experiments required to obtain estimates with an error tolerance given by* δ *and using* $\varepsilon = 0.005$.

δ	ordinary Chebyshev $\log N$	exponential Chebyshev $\log N$
0.001	7.0	5.18
0.005	6.3	5.07
0.01	6.0	5.02
0.05	5.3	4.86
0.1	5.0	4.77

not. Therefore, we can think of the computation of form factors as a Bernoulli trial, and the sample rays as Bernoulli random variables, since all rays are generated independently and according to the same distribution. Viewed in this context, the form factor F_{ij} linking an emitter element i and a receiver element j, or the probability that a sample ray sent by the emitter hits the receiver, corresponds to p. Also, the total number of sample rays N corresponds to k, and the number of rays m that hit the receiver element corresponds to S_k. Therefore, Eqs. (27) and (33), and the respective bounds derived from them, can be rewritten and applied to the computation of form factors. In this case Eq. (33) can be rewritten as:

$$P\left\{\left|\frac{m}{N} - F_{ij}\right| < \varepsilon\right\} \geq 1 - 2e^{-2N\varepsilon^2} \tag{37}$$

and the bound on the number of sample rays derived from the exponential Chebyshev inequality is given by:

$$N = \left\lceil \frac{\ln(\frac{2}{\delta})}{2\varepsilon^2} \right\rceil \tag{38}$$

3.3. Selection of Parameters

The application of the proposed bound for ray density, as shown by Eq. (38), requires the selection of only two parameters, namely the error tolerance δ with respect to the estimand and a strip of width ε, henceforth referred as uncertainty. The choice of error tolerance is highly dependent on the application. For example, as mentioned by Nievergelt [33], illuminating engineers need radiative transfer solutions accurate to only 1% to 10%, since humans do not perceive finer variations of light. In order to evaluate the applicability of the proposed bound (Sec. 5), we selected a value for the error tolerance in the low end of this range, *i.e.* $\delta = 0.01$. The selection of an error tolerance few orders of magnitude higher or lower would not affect our observations considerably, since, as shown by the figures presented in Table 1, the proposed bound based on the exponential Chebyshev inequality is not as sensitive to changes in the error tolerance as the bound derived from the ordinary Chebyshev inequality.

The selection of a value for the uncertainty ε depends on how deep in the region of convergence one wants the estimates to be. By using very small values for ε, we can obtain estimates within the region of constant convergence. In this case, however, the time measurements presented in the next section show that the corresponding reliability/cost ratios will be significatively lower due to a significative increase in the computational times. Therefore, we need to select a value for ε that provides an acceptable trade-off between reliability and processing time.

Consider the following geometrical ratio given by:

$$K = A/d \tag{39}$$

where A corresponds to the area of the receiver element, and d corresponds to the distance between the emitter and the receiver. Clearly, if the value of K is smaller, the value of the form factor linking the elements will be smaller as well, since, as pointed out by Howell [34], a small fraction of the total number of rays would strike the receiver. This aspect indicates that an optimal choice for ε should take into account the magnitude of the estimand. For example, consider $\varepsilon = 0.01$ and assume that the value of the estimand is 0.2. In this case, as indicated in Eq. (23), the choice of $\varepsilon = 0.01$ would be appropriate to obtain estimates with a magnitude of approximately 0.2 ± 0.01 with a probability of $1 - \delta$. However, by reducing the area of the receiver, we have a reduction in the value of the estimand. In this case, assuming that the value of the estimand is 0.02 and using $\varepsilon = 0.01$, we can expect estimates with a magnitude of approximately 0.02 ± 0.01 with a probability of $1 - \delta$, *i.e.* estimates with a deviation that may reach 50% of the value of the estimand.

Obviously, we cannot propose a strategy for selecting ε based on the estimand, since, as mentioned earlier, we do not know *a priori* its value. Nevertheless, we know that the form factors take values in the interval $[0.1]$, whose mean corresponds to 0.5. Moreover, a standard deviation of approximately 1%, or 0.01, is considered satisfactory for radiative transfer applications [34, 35]. Using these figures, we may select a value for the uncertainty given by $\varepsilon \leq 0.5 \times 0.01 = 0.005$. The experiments presented in Sec. 5 revealed that by setting $\varepsilon = 0.005$ we can obtain meaningful estimates with reasonably high reliability/cost ratio. Our experiments also suggest that ε should be less than K, otherwise, for the reason described above, we cannot ensure a low deviation of the estimates with respect to the estimand. Hence, for geometries in which $\varepsilon > K$, we propose the reduction of ε by one order of magnitude. The use of this heuristic procedure to select ε allows us to obtain reliable and meaningful estimates even for geometries in which K presents a very small value, as borne out by the experiments presented in Sec. 5.

4. Experimental Issues

4.1. Performance Criterion

Farmer and Howel [36] define the "performance" of a Monte Carlo based method as:

$$performance = \nu^2 t \tag{40}$$

where ν^2 corresponds to the variance of the solution, and t corresponds to the processing time. As stated by Howel [34], the method or strategy in a Monte Carlo simulation that minimizes the value of the quantity given by equation Eq. (40) is assumed to be the best choice.

Since, in this paper, instead of different Monte Carlo based methods, we are comparing different choices for ray density, which are intentionally not based on the knowledge about the variance, we found more appropriate to use a slightly different "performance" criterion in our comparisons. Recall that our main goal is to obtain estimates with a high reliability/cost ratio, which we define as:

$$reliability/cost = \frac{(1-\delta)(1-\varepsilon)}{t} \tag{41}$$

For the sake of fairness, we consider the same value for the error tolerance δ and for the uncertainty ε in our comparisons involving different ray density bounds. Therefore, the bound that provides the smallest number of rays and, consequently, the shortest processing time, is considered to be the best choice, since it minimizes the quantity given by Eq. (41).

4.2. Geometrical Configurations and Analytical Formulae

In order to demonstrated the applicability of the proposed bound, we have computed the form factors for a number of geometrical configurations using a nondeterministic method as outlined in Sec. 2. Without loss of generality, we selected geometries for which analytical formulae for the corresponding form factors are known. This aspect allowed us to compare the numerical estimates with the analytical values and ensure the correctness of the algorithms used in our experiments. Notice that the estimand for a given geometrical configuration does not need to be identical to the corresponding analytical form factor. After all, this estimand is associated with an stochastic numerical process. For the sake of completeness, however, we included in the next section comparisons between numerical estimates and analytical values for the geometrical configurations used in our experiments. These comparisons illustrate the accuracy of the nondeterministic computation of form factors, and were performed through the computation of the relative deviation of the numerical estimates, with respect to the corresponding analytical values, using the following expression:

$$r.d.(\%) = \frac{|analytical\ value - numerical\ estimate|}{|analytical\ value|} \times 100 \tag{42}$$

with the figures for analytical and numerical form factors truncated after the seventh digit.

4.2.1. Differential Element to Right Triangle

The first geometrical configuration used in our experiments corresponds to a form factor linking a differential element dA_i to a right triangle A_j in a plane parallel to the plane of dA_i, with the normal of dA_i passing through a vertex of A_j. (Fig. 1). The analytical form factor for this configuration is given by the following expression found in Ref. 9:

$$F_{ij} = \frac{X}{2\pi(1+X^2)^{\frac{1}{2}}}\ tan^{-1}\left(\frac{X\ tan\theta}{(1+X^2)^{\frac{1}{2}}}\right) \tag{43}$$

where X is given by:

$$X = \frac{a}{b} \tag{44}$$

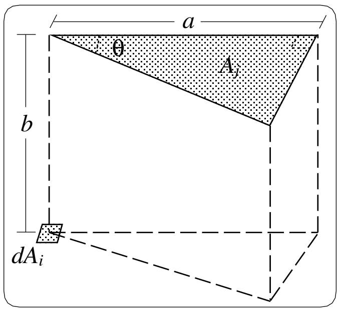

Fig. 1: *Differential element to right triangle.*

4.2.2. Differential Element to Parallel Polygon

The second geometrical configuration used in our experiments corresponds to a form factor linking a differential element dA_i to a parallel polygon A_j, with the normal of dA_i passing through a corner of A_j (Fig. 2a). The analytical form factor for this configuration is given by the following expression found in Ref. 5:

$$F_{ij} = \frac{1}{2\pi}\left[\frac{a}{(a^2+c^2)^{\frac{1}{2}}}\ sin^{-1}\left(\frac{b}{(a^2+b^2+c^2)^{\frac{1}{2}}}\right) + \frac{b}{(b^2+c^2)^{\frac{1}{2}}}\ sin^{-1}\left(\frac{a}{(a^2+b^2+c^2)^{\frac{1}{2}}}\right)\right] \tag{45}$$

4.2.3. Differential Element to Perpendicular Polygon

The third geometrical configuration used in our experiments corresponds to a form factor linking a differential element dA_i to a polygon A_j in a plane perpendicular to the plane of dA_i, with dA_i lying in a plane through one edge of A_j and with its normal passing through a corner of the polygon (Fig. 2b). The analytical form factor for this configuration is given by another expression found in Ref. 5:

$$F_{ij} = \frac{1}{2\pi}\left[sin^{-1}\left(\frac{a}{(a^2+c^2)^{\frac{1}{2}}}\right) - \frac{c}{(b^2+c^2)^{\frac{1}{2}}}\ sin^{-1}\left(\frac{a}{(a^2+b^2+c^2)^{\frac{1}{2}}}\right)\right] \tag{46}$$

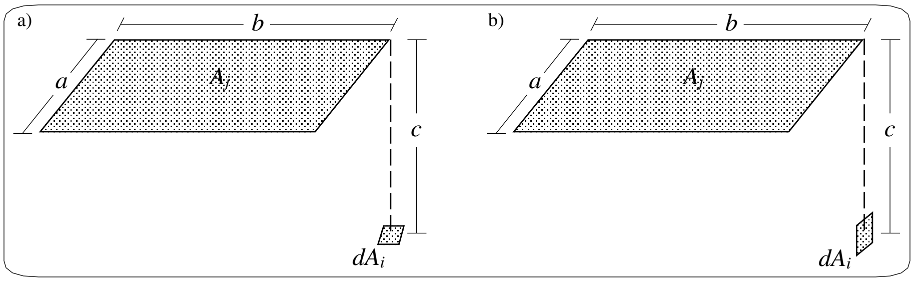

Fig. 2: *a) Differential element to parallel polygon. b) Differential element to perpendicular polygon.*

4.2.4. Differential Element to Coaxial Sphere

The fourth geometrical configuration used in our experiments corresponds to a form factor linking a differential element dA_i to a sphere A_j, with the normal of dA_i passing through the center of A_j (Fig. 3a). The analytical form factor for this configuration is given by the following expression found in Refs. 2 and 7:

$$F_{ij} = \left(\frac{r}{h}\right)^2 \tag{47}$$

4.2.5. Differential Element to Perpendicular Sphere

The fifth geometrical configuration used in our experiments corresponds to a form factor linking a differential element dA_i to a sphere A_j, with dA_i lying in a plane perpendicular to A_j axis (Fig. 3b). The analytical form factor for this configuration is given by the following expression found in Refs. 3 and 7:

$$F_{ij} = \frac{H}{(L^2+H^2)^{\frac{3}{2}}} \tag{48}$$

for $H \geq 1$, and with L and H given by:

$$L = \frac{l}{r} \quad and \quad H = \frac{h}{r} \tag{49}$$

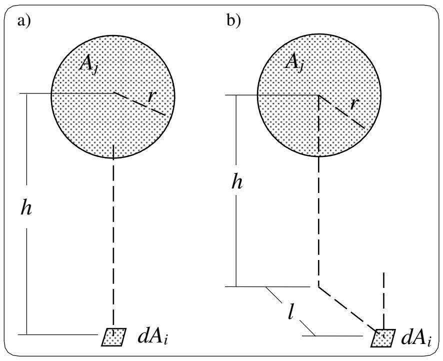

Fig. 3: *a) Differential element to coaxial sphere. b) Differential element to perpendicular sphere.*

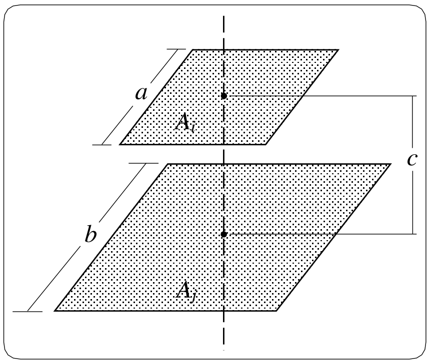

Fig. 4: *Two unequal, parallel coaxial squares.*

4.2.6. Square to Parallel Coaxial Square of Differing Size

Finally, the sixth geometrical configuration used in our experiments corresponds to the form factor between two unequal, parallel coaxial squares A_i and A_j (Fig. 4). The analytical form factor for this configuration is given by the following expression found in Ref. 4:

$$\begin{aligned} F_{ij} = \frac{1}{\pi A^2}\Bigg\{\ln\left(\frac{[A^2(1+B^2)+2]^2}{(Y^2+2)(X^2+2)}\right) \quad & +(Y^2+4)^{\frac{1}{2}}\left[Y\ tan^{-1}\left(\frac{Y}{(Y^2+4)^{\frac{1}{2}}}\right) - X\ tan^{-1}\left(\frac{X}{(Y^2+4)^{\frac{1}{2}}}\right)\right] \\ & +(X^2+4)^{\frac{1}{2}}\left[X\ tan^{-1}\left(\frac{X}{(X^2+4)^{\frac{1}{2}}}\right) - Y\ tan^{-1}\left(\frac{Y}{(X^2+4)^{\frac{1}{2}}}\right)\right]\Bigg\} \end{aligned} \tag{50}$$

for $A \geq 0.2$, and with X and Y given by:

$$X = A(1+B) \quad and \quad Y = A(1-B) \tag{51}$$

where A and B are given by:

$$A = \frac{a}{c} \quad and \quad B = \frac{b}{a} \tag{52}$$

5. Results and Discussion

Applying to the proposed bound (Eq. (38)) with $\delta = 0.01$ and $\varepsilon = 0.005$, as suggested in Sec.3.3, results in a ray density given by $N = 10^{5.02}$ (or $logN = 5.02$). Figures 5-10 present the form factor estimates as well as the time measurements (given by elapsed CPU time on a SGI R5000) for the application of a nondeterministic method, as outlined in Sec. 2, to the computation of the form factors associated with geometries described in the previous section. For each graph presented in Figs. 5a-10a and in Fig. 12 we use a scale for the x and y axes such that we can observe the peaks and the full convergence history of the estimates. As we can see in the graphs presented in Figs. 5a-10a, the estimates obtained using $N = 10^{5.02}$ (or $logN = 5.02$) are within the region of asymptotic convergence of the form factors.

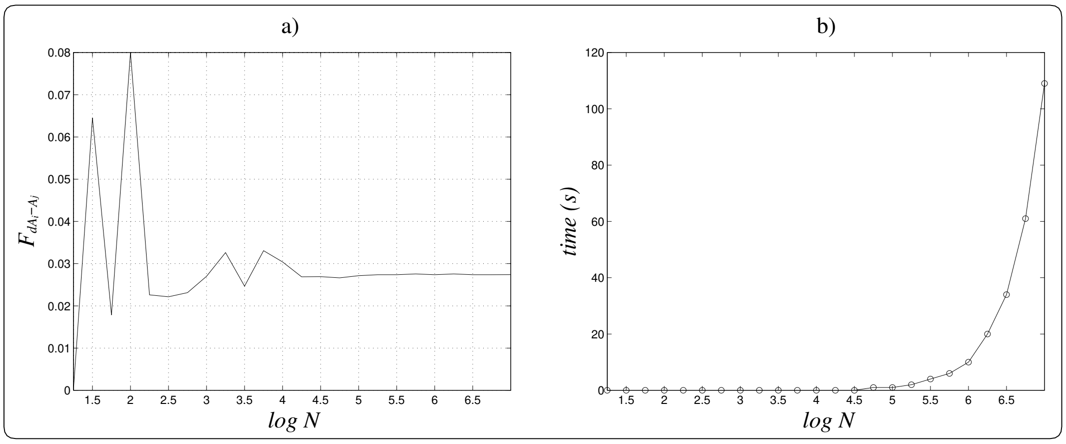

Fig. 5: *Experiments for the form factor linking a differential element to a right triangle: a) form factor estimates, and b) time measurements. For this geometrical configuration we set $a = 2$, $b = 3$ and $\theta = 30^\circ$, which, using Eq. (43), results in an analytical form factor equal to* 0.0273621.

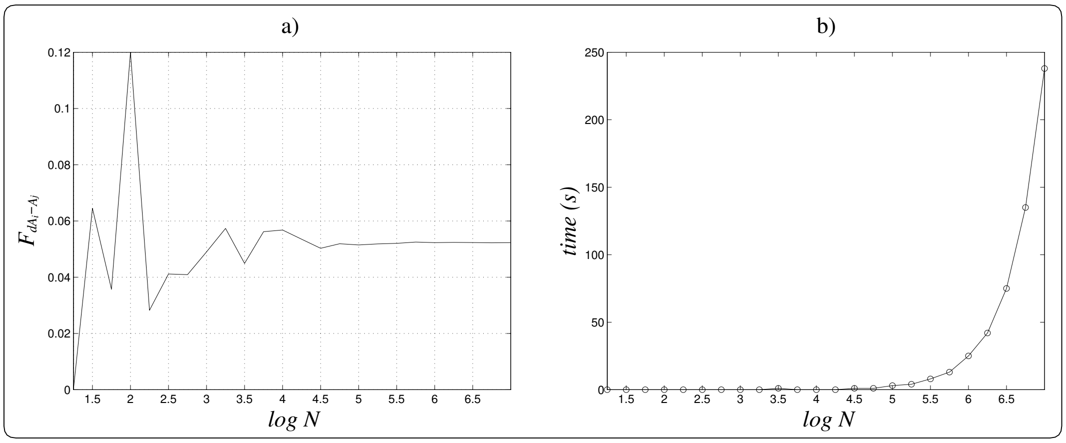

Fig. 6: *Experiments for the form factor linking a differential element to a parallel polygon: a) form factor estimates, and b) time measurements. For this geometrical configuration we set $a = 1$, $b = 2$ and $c = 3$, which using Eq. (45), results in an analytical form factor equal to* 0.0522678.

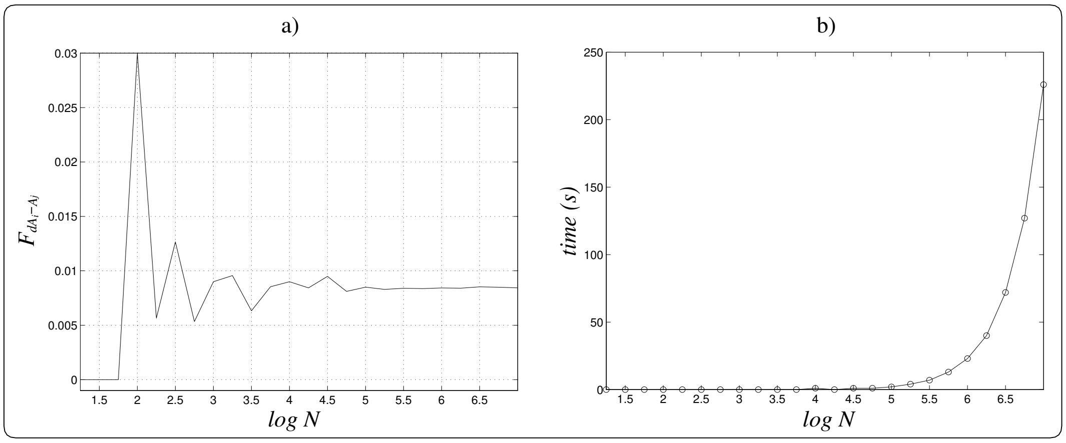

Fig. 7: *Experiments for the form factor linking a differential element to a perpendicular polygon: a) form factor estimates, and b) time measurements. For this geometrical configuration we set $a = 2$, $b = 1$ and $c = 3$, which using Eq. (46), results in an analytical form factor equal to* 0.0084414.

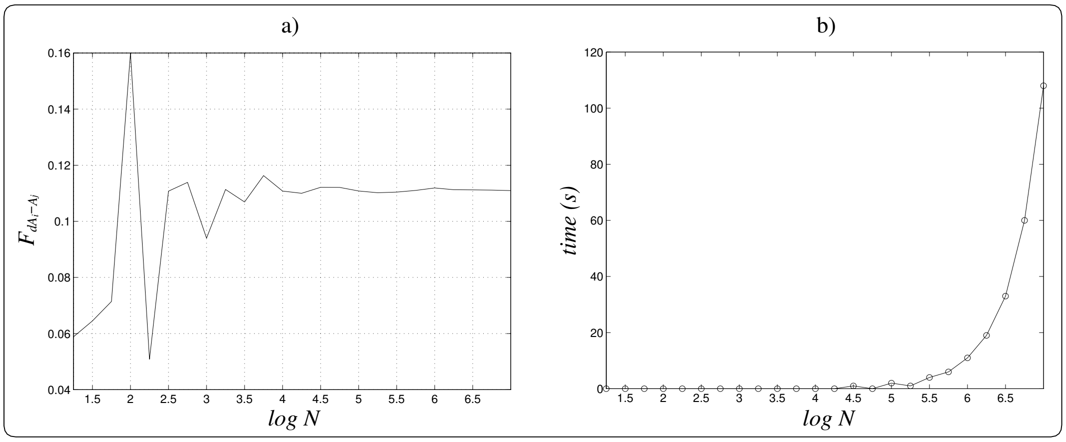

Fig. 8: *Experiments for the form factor linking a differential element to a coaxial sphere: a) form factor estimates, and b) time measurements. For this configuration we set $r = 1$ and $h = 3$, which, using Eq. (47), results in an analytical form factor equal to* 0.1111111.

Notice that with the application a brute-force approach, *e.g.* using $N = 10^7$ (or $\log N = 7$), we could obtain estimates within the region of constant convergence. The graphs regarding the time measurements presented in Figs. 5b-10b show, however, that in this case we would have a very significant increase in the processing time required by the nondeterministic method to compute the form factors. This aspect suggests, therefore, that we can obtain estimates with a much higher reliability/cost ratio using a number of rays provided by a bound based on probability theory (Sec. 3). Moreover, by examining the figures presented in Table 1, for $\varepsilon = 0.005$ and $\delta = 0.01$, and the graphs for the time measurements presented in Figs. 5b-10b, we can also verify that the more precise proposed bound, derived from the exponential Chebyshev inequality, allows us to obtain estimates with a higher reliability/cost ratio than the bound derived from the ordinary Chebyshev inequality.

The practical benefit of using a tighter bound becomes even more noticeable when one works with applications involving a large number of form factor computations, *e.g.* applications involving radiative transfer simulations between moving objects. Recall that in the experiments presented in this paper we are dealing with static geometries only. In more complex simulations we may, however, have dynamic geometrical configurations. For example, suppose that we want to determine the radiation transfer from a star or planet to a spacecraft or satellite [37, 38] (Fig. 11). In this case, we need to compute the form factor between the elements at each selected point of the objects' trajectories. Depending on the resolution chosen for the simulation, we may

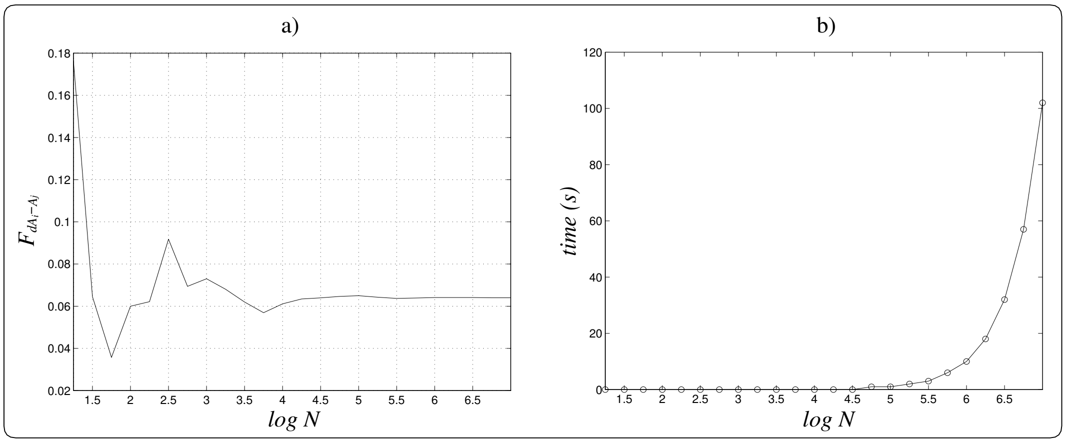

Fig. 9: *Experiments for the form factor linking a differential element to a perpendicular sphere: a) form factor estimates, and b) time measurements. For this geometrical configuration we set $r = 1$, $l = 2$ and $h = 3$, which, using Eq. (48), results in an analytical form factor equal to* 0.0640038.

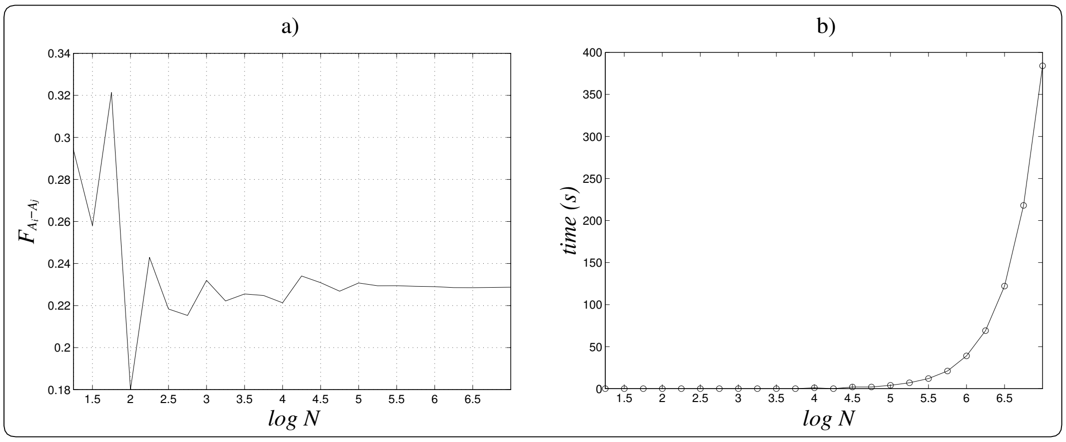

Fig. 10: *Experiments for the form factor linking two unequal, parallel coaxial squares: a) form factor estimates, and b) time measurements. For this geometrical configuration we set $a = 2$, $b = 4$ and $c = 4$, which, using Eq. (50), results in an analytical form factor equal to* 0.2284608.

need to perform hundreds, or even thousands, of form factor computations. For these situations the computational savings provided by the application of the tighter proposed bound would be highly significant, reducing the total processing time by several orders of magnitude.

Figure 12 presents additional experiments for the form factor linking two unequal, parallel coaxial squares. For these experiments the geometrical parameters were specifically selected to allow the analysis of the suitability of the proposed bound for small values of K. The graph of form factor estimates presented in Fig. 12a indicates that the choice of $\varepsilon = 0.05$, which, by applying the proposed bound with $\delta = 0.01$ results in $N = 10^{5.02}$ (or $logN = 5.02$), is appropriate to obtain reliable and meaningful form factor estimates for this geometrical configuration in which $K = 0.0625$. However, the graph of form factor estimates presented in Fig. 12b shows that, as mentioned in Sec. 3.3, when we select a value for the uncertainty such that $\varepsilon > K$, the ray density provided by the proposed bound is insufficient to obtain meaningful estimates. In this case, if we reduce the value assigned to ε by one order of magnitude such that $\varepsilon = 0.0005 < K$, as also suggested in Sec. 3.3, we obtain, by applying the proposed bound with $\delta = 0.01$, a ray density given by $N^{7.02}$ (or $logN = 7.02$). As we can see in Fig. 12b, this ray density is appropriate to obtain reliable and meaningful estimates for this geometrical configuration in which $K = 0.000625$.

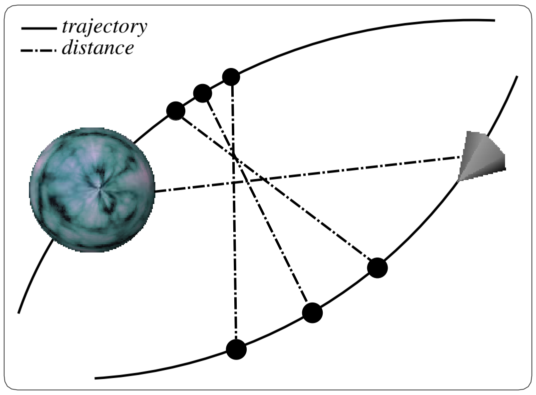

Fig. 11: *Sketch of an application involving moving objects.*

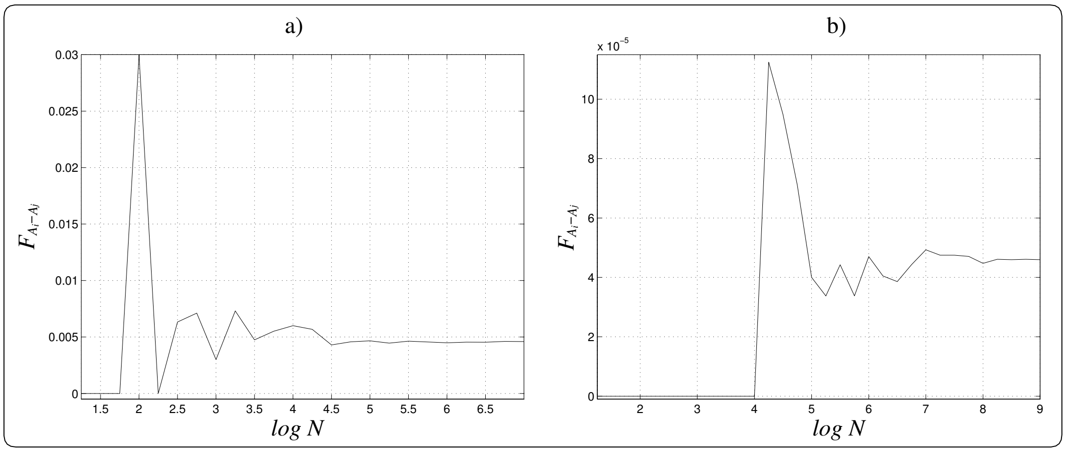

Fig. 12: *Estimates for the form factor linking two unequal, parallel coaxial squares: a) using* $a = 2$*,* $b = 0.5$ *and* $c = 4$*, which results in* $K = 0.0625$*, and b) using* $a = 2$*,* $b = 0.05$ *and* $c = 4$*, which results in* $K = 0.000625$*.*

As mentioned in Sec. 3.3, in our experiments the error tolerance of the estimates, which are obtained through a stochastic numerical process, is given with respect to the estimand of the numerical form factors. Hence, a formal relationship with analytical values for the form factors cannot established, despite the fact that one can intuitively assume that the estimands of numerical form factors and the corresponding analytical form factors shall be very close. Nevertheless, the accuracy of the nondeterministic method used in our experiments to compute these estimates can be verified upon the observation that the numerical estimates computed for each geometrical configuration converge to the analytical values associated with these configurations. Moreover, the figures presented in Table 2 indicate that, using a ray density given by the proposed bound, we may obtain estimates with a reasonably low deviation with respect to the analytical values. Notice that the generation of uniformly distributed random numbers during the stochastic process was performed using pseudo-random number generators, which in our experiments corresponds to the standard function `rand()` [39]. The use of a more elaborated function, with wider spectral properties, *e.g.* `drand48()` [39], may reduce the relative deviations presented in Table 2, although it would likely introduce an additional computational overhead as well.

Table 2: *Relative deviation of the numerical estimates, obtained using a ray density given by* $10^{5.02}$ *(or* $logN = 5.02$*) derived from the exponential Chebyshev inequality, with respect to the analytical form factors for the geometrical configurations used in our experiments.*

geometrical configuration	$r.d.(\%)$
differential element to a right triangle	0.77
differential element to a parallel polygon	1.48
differential element to a perpendicular polygon	0.69
differential element to a coaxial sphere	0.26
differential element to a perpendicular sphere	1.54
two unequal, parallel coaxial squares (with $K = 4$)	0.99

6. Conclusion

The computation of form factors represents the kernel of radiative transfer simulations. Numerical nondeterministic methods are often used in these simulations due to their simplicity and generality for application to complex geometries. These methods implicitly compute form factors using Monte Carlo sampling techniques and ray casting algorithms. As pointed out by Howell [34], because of their accurate treatment of complex geometries, Monte Carlo based methods are often used to validate results provided by other methods, and are likely to become the dominant choice for treating radiative transfer problems. Their accuracy, however, depends heavily on the ray density used in the computations, and an over dimensioned density may result in a high computational cost in terms of processing time. The main problem is, therefore, to determine the least number of sample rays required to obtain reliable estimates with respect to the constraints of radiative transfer simulations, and to keep the computational costs as low as possible.

In this paper we presented a bound for the ray density required to compute estimates for form factors between diffuse elements with a high reliability/cost ratio. This bound was derived from a probability concept, namely the exponential Chebyshev inequality. Besides its contribution to a better theoretical foundation for the nondeterministic computation of form factor, its application results in substantial computational time savings. For simulations involving moving objects, which involve the computation of form factors for several instances of the parameters associated with a given geometrical configuration, we believe that, by applying the proposed bound, the total computational time may be reduced by several orders of magnitude.

Our future efforts in this area will be focus on the application of the proposed bound to other problems involving particle transport simulation such as virtual spectrophotometry and goniophotometry. Moreover, we intend to look more closely at the application of parallel techniques to the computation of form factors through nondeterministic methods. Clearly, these methods are suitable for parallelization, and there are several different parallel approaches that can be used to obtain an approximately linear speed up in radiative transfer applications involving Monte Carlo based methods [40, 34]. After all, by simply dividing the total number of rays among a certain number of processors, one may reduce considerably the processing time. Notice that, before using a parallel approach, one shall determine the least number of rays required to obtain reliable results in an efficient sequential implementation. This aspect reinforces the importance of the proposed bound, which fulfill this requirement as illustrated by the numerical experiments presented in this paper.

References

1. M.F. Modest. *Radiative Heat Transfer*. McGraw-Hill, New York, 1993.

2. B.T.F. Chung and P.S. Sumitra. Radiation shape factors from plane point sources. *ASME Journal of Heat Transfer*, 94(3):328–330, August 1972.

3. B.T.F. Chung and M.H.N. Naraghi. Some exact solutions for radiation view factors from spheres. *AIAA Journal*, 19(8):1077–1081, August 1981.

4. M. Crawford. Configuration factor between two unequal, parallel coaxial squares. *ASME paper n. 72-WA/HT-16*, November 1972.

5. H.C. Hottel and A.F. Sarofim. *Radiative Transfer*. McGraw-Hill Book Company, 1967.

6. J.R. Howell. *A Catalog of Radiation Heat Transfer Configuration Factors*, 1998. Eletronic version available at http://sage.me.utexas.edu/ howell/index.html.

7. N.H. Juul. Diffuse radiation view factors from differential plane sources to spheres. *ASME Journal of Heat Transfer*, 101(3):558–560, August 1979.

8. P. Schroder and P. Hanrahan. On the form factor between two polygons. In *SIGGRAPH Proceedings, Annual Conference Series*, pages 163–164, 1993.

9. R. Siegel and J.R. Howell. *Thermal Radiation Heat Transfer*. Hemisphere Publishing Corporation, Washington, second edition, 1981.

10. E.M. Sparrow and R.G. Cess. *Radiation Heat Transfer*. Brooks/Cloe, Belmont, 1966.

11. J.A. Wiebelt. *Engineering Radiation Heat Transfer*. Holt Rinehart and Winston, New York, 1966.

12. G.V.G. Baranoski. The parametric differential method: An alternative to the calculation of form factors. *Computer Graphics Forum (EUROGRAPHICS Proceedings)*, 11(3):193–204, September 1992.

13. J.M. Hammerley and D.C. Handscomb. *Monte Carlo Methods*. Wiley, New York, 1964.

14. A. Appel. Some techniques for shading machine renderings of solids. In *Spring Joint Computer Conference*, pages 37–45, 1968.

15. G.M. Maxwell, M.J. Bailey, and V.W. Goldschmidt. Calculations of the radiation configuration factor. *Computer-aided Design*, 18(7):371–379, September 1986.

16. A.N. Shiryaev. *Probability*. Springer-Verlag, New York, second edition, 1996.

17. H. Gordon. *Discrete Probability*. Springer-Verlag, New York, 1997.

18. C.L. Chiang. *An Introduction to Stochastic Processes and Their Applications*. Robert E. Krieger Company, New York, 1980.

19. B.W. Lindgren. *Statistical Theory*. The Macmillan Company, New York, 1962.

20. M. Pellegrini. Monte Carlo approximation of form factor with error bounded a priori. In *Eleventh ACM Symposium on Computational Geometry*, pages 287–296, Vancouver, June 1995.

21. L.A. Santaló. *Integral Geometry and Geometric Probability*. Addison-Wesley, Reading, M.A., 1976.

22. P. Shirley. *Physically based lighting for computer graphics*. PhD thesis, Dept. of Computer Science, University of Illinois, November 1990.

23. R.S. Longhurst. *Geometrical and Physical Optics*. Longman Group Limited, London, third edition, 1973.

24. P. Shirley. Radiosity via ray tracing. In *Graphics Gems II*, pages 306–310. Ed. Academic Press, 1991.

25. P. Shirley. Time complexity of Monte Carlo radiosity. In F.H. Post and W. Barth, editors, *Proceedings of the Annual Conference of the European Association for Computer Graphics - EUROGRAPHICS*, pages 459–465, Amsterdam, 1991. North-Holland.

26. D.W. Yarbrough and L. Chon-Lin. Monte Carlo calculation of radiation view factors. In F.R. Payne, C.C. Corduneanu, A. Haji-Sheikh, and T. Huang, editors, *Integral Methods in Science and Engineering*, pages 563–574, Washington, 1986. Hemisphere.

27. P. Shirley. Nonuniform random points via warping. In D. Kirk, editor, *Graphics Gems III*, pages 80–83. Academic Press, 1992.

28. E.P. Lafortune and Y. D. Willems. Using the modified phong reflectance model for physically based rendering. Technical report, Department of Computer Science, K.U. Leuven, November 1994.

29. B.R. Frieden. *Probability, Statistical Optics, and Data Testing: A Problem Solving Approach*. Springer-Verlag, New York, 1983.

30. J.V. Uspensky. *Introduction to Mathematical Probability*. McGraw-Hill, New York, 1937.

31. E.D. Cashwell and C.J. Everett. *A Practical Manual on the Monte Carlo Method for Random Walk Problems*. Pergamont Press, New York, 1959.

32. L. Carter and E.D. Cashwell. Particle transport simulation with the Monte Carlo method. Technical report, Energy Research and Development Administration, 1975.

33. Y. Nievergelt. Radiosity in illuminating engineering. *The UMAP Journal*, 18(2):167–179, 1997.

34. J.R. Howell. The Monte Carlo method in radiative heat transfer. *Journal of Heat Transfer*, 120:547–560, August 1998.

35. P.P. Almazan. Accuracy control in Monte Carlo radiative calculations. In *Fifth Annual Thermal and Fluids Analysis Workshop*, pages 47–62, Ohio, August 1993. NASA Conference Publication 10122.

36. J.T. Farmer and J.R. Howell. Monte Carlo strategies for radiative transfer in participating media. In J.P. Hartnett and T. Irvine, editors, *Advances in Heat Transfer*, Vol. 31, pages 333–429, San Diego, 1998. Academic Press.

37. J.F. Baumeister. Application of ray tracing in radiation heat transfer. Technical Report NASA TM-106206, NASA Lewis Research Center, Cleveland, Ohio, 1993. Prepared for the Computer Applications Symposium cosponsored by the ASME and LMU (Los Angeles, California, March, 1993) and Thermal and Fluids Analysis Workshop sponsored by NASA Lewis Research Center (Cleveland, Ohio, August 1993).

38. E. Golliher. A comparison of TSS and TRASYS in form factor calculation. In *Fifth Annual Thermal and Fluids Analysis Workshop*, pages 41–46, Ohio, August 1993. NASA Conference Publication 10122.

39. C. D. Petersen. *Xman*. Massachusetts Institute of Technology, 1988. Version 3.1.5 - X11R5.

40. J.F. Farmer. *Improved Algorithms for Monte Carlo Analysis of Radiative Heat Transfer in Complex Participating Media*. PhD thesis, Faculty of Graduate School, The University of Texas at Austin, August 1995.